IJESRT

INTERNATIONAL JOURNAL OF ENGINEERING SCIENCES & RESEARCH TECHNOLOGY

ANN-Based Approach for Fault Detection in GIS.

Ebrahim A. Badran[*1], Mansour H. Abdel-Rahman[2], Mohamed Hamed Abdel-Rahim[3]

[*1,2]Electrical Engineering Department, Faculty of Engineering, Mansoura University, Mansoura, Egypt

[3]Middle Delta Company for Electricity Production, Talkha, Egypt

ebadran@hotmail.com

Abstract

This paper introduces an artificial neural network (ANN) approach for fault detection in gas insulated substation (GIS). Faults in GIS have to be located and classified as soon as possible to start the processes of reconfiguration and restoration of the normal power supply. A practical case study is analyzed using Talkha 220KV GIS, which represents a critical generation point in the Egyptian Electric Power Network. Firstly, the layout of the Talkha 220 kV GIS is discussed and modeled using ATP/EMTP. Secondly, the ANN is built and trained. Finally, the proposed approach is tested using solidly grounded faults and high impedance faults. The results ensure the success of the proposed approach to locate and classify any fault in and/or out the GIS.

Keywords: GIS, ANN, Fault detection, ATP/EMTP.

Introduction

In power system substations, faults that produced load disconnections or emergency situations have to be located as soon as possible. Faults location is necessary to start the substation reconfiguration for restoring normal energy supply. Failures in GIS are known to have occurred both during early years of operation and during site testing or assembling. From the statistical point of view, problems have occurred at the highest voltage levels rather than the lower level [1]. However, the identification of the faulted points is not always an easy task, delaying the restoration procedures. This usually occurs when the protection system does not behave as expected. Substation in commissioning phase or even the ones already in operation, but with complex constructive and operational natures, can have high indices of protection system failure. In these substations, fault location can take a long time due to the great amount of information to be analyzed. The difficulty in identifying the fault points significantly increases in non-conventional substation, as gas-insulated ones [2].

In GIS a large number of restrikes occur across the switching contacts when disconnector, breaker operations, the closing of grounding switch, and by line-to-ground faults. Each strike leads to generation of a Very Fast Transient (VFT) [2]. The generation and propagation of VFT from their original location throughout a GIS can produce internal and external overvoltages. In case of a line-to-ground fault, the voltage collapse at the fault location occurs in a similar way as in the disconnector gap during striking. Step-shaped traveling surges are generated and injected to GIS lines connected to the collapse location [3].

VFT in GIS can be divided into internal and external. Internal transients can produce overvoltages between inner conductors and the encapsulation, external transients can cause stress on secondary and adjacent equipment. Breakdown phenomena across the contacts of a disconnector during a switch operation or line-to-ground faults generate very short rise time traveling waves which propagate in either direction from the breakdown or fault location. Surges traveling throughout GIS and to other connected equipment are reflected and refracted at every transition point. As a consequence of multiple reflections and refractions, traveling voltages can increase above the original values and very high frequency oscillations occur. An internally generated VFT propagates throughout the GIS and reaches the bushing where it causes a transient enclosure voltage and a traveling wave that propagates along the overhead transmission line [2].

In the areas of power systems, problems may have one or more of the following characteristics: dynamic, non-linear, large scale and random like. These factors make power system problems more difficult to solve. Therefore, computers are extensively applied to power system operation, planning, monitoring and control. Current

approaches to power system computation are mainly based either on developing a mathematical model of a relevant part of the system or on expert systems. ANNs provide a promising and attractive alternative [4].

ANNs have the inherent capacity of modeling functional relationships between input and output data without the explicit knowledge of an analytical model. ANNs have a great pattern recognition capabilities and their ability to handle noisy data. There are widespread applications of ANNs in a number of different areas of power systems such as: load forecasting, security assessment, control, system identification, protection, fault location, adaptive auto reclosing, operational planning, etc. Matlab/Simulink has a suite of programs designed to build ANNs (Neural Networks Toolbox) [5]. There are three steps to using ANNs; design, training, and testing [6-7].

This paper concerns the fault identification and detection in GIS. A practical case study is analyzed using Talkha 220 kV GIS. This GIS represents a critical generation point in the Egyptian Electric Power Network. Firstly, the layout of the Talkha 220 kV GIS is discussed and modeled using ATP/EMTP. Secondly, the ANN is built and trained. Finally, the proposed approach is tested using solidly ground faults and high impedance faults.

Talkha 220 kV GIS

Talkha 220 kV GIS is an important generation busbar in the north of Egypt. The fault in GIS at this point in the Egyptian power network may lead to severe stability events that may result in a complete or partial blackout. So, attention must be given to prevent or limit fault consequences. A typical 220 kV GIS installation of a one-and-half circuit breaker arrangement is used in this paper as a case study. It consists of circuit breakers, disconnectors, busbars, surge arresters, transmission lines, transformers, generators, coupling feeders, earthing switches.

Fig. 1 illustrates the construction of Talkha 220 kV GIS. It consists of eight bays; each with three circuit breakers, six disconectors, six current transformers, and eight earthing switches. The GIS system contains two busbars which are supplied from seven generation sources using two 150 MVA delta/star 11.5/220 kV transformers, two 200 MVA star/star 11.5/220 kV transformers, and three 320 MVA delta/star 16.5/220 kV transformers which supplies a 66 kV substation through five 125 MVA, 220/70 kV star/star transformers, and six transmission lines which connect the GIS to the surrounding substations.

. Modeling of Talkha 220 kV GIS

Due to the traveling wave nature of the VFT, the GIS elements are modeled as electrical equivalent circuits composed of distributed parameter lines (defined by surge impedance and traveling times) as well as lumped elements. In order to achieve reliable simulation results the GIS is subdivided into several shorter sections. Table 1 gives the GIS components and how to be modeled [2], [8].

The GIS installation is regarded as series of distributed parameters transmission lines and lumped capacitor elements. The values of each GIS section are calculated from the standard formula of capacitance. The Capacitance is calculated with the assumption that the conductors are cylindrical [9]. Capacitance is calculated by the following [3], [10];

$$C = 2\pi\varepsilon_o\varepsilon_r l \Big/ 2.3\ln\left(b/a\right) \quad (1)$$

where b is the outer cylinder radius, a is the inner cylinder radius, and l is the length of the section. Spacers are used for supporting the inner conductor with reference to the outer enclosure. They are made with Alumina filled epoxy material whose relative permittivity, ε_r, is 4. The thickness of the spacer is assumed to be the length of the capacitor which is taken as 15~1000 pF.

The gas insulated busbar is represented by the surge impedance, the velocity of surge propagation, and the length. The surge impedance of a gas insulated bus bar is calculated from the relation [9]:

$$Z = 60 \times \ln\left(B/A\right) \quad (2)$$

where A is the diameter of the bus and B is the inner diameter of the enclosure. The surge impedance of the 220 kV busbar is taken as 90 Ω and the surge velocity is assumed be the velocity of light.

Fig. 2 illustrates the ATP/EMTP model of the 220 kV TALKHA GIS. In this model each Bay consists of three partitions and each partition has six sections. So the fault can be applied at eighteen points for each Bay in the GIS

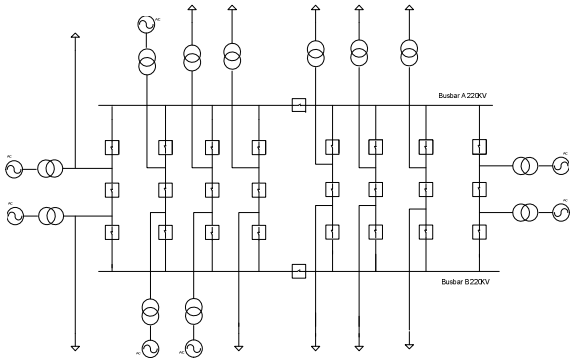

220 kV Transmission Lines

Fig. 1. A typical single line diagram of Talkha 220kV GIS

Table 1. Models of GIS Components

GIS Component		Equivalent Circuit
Circuit Breaker	Open	Distributed parameters transmission line in series with grading
	Close	Distributed parameters transmission line
Busbar		Distributed parameters transmission line
Earthing Switch		Lumped capacitor to earth
Disconnector	Open	Distributed parameters transmission line in series with capacitor
	Close	Distributed parameters transmission line

4. Simulation of Faults in GIS

Faults in GIS are modeled using single-line-to-ground fault with two types; solidly to ground (SLG) and high impedance fault (HIF). The arc of HIF is modeled usir BB#2 s in combination with TACS in ATP/EM] e arc model is based on the energy balance of the arc and describes an arc in air by a differential equation of the arc conductance (g) [12]. Fig. 3 illustrates the main components of the HIF arc model using ATP/EMTP.

Fig. 4 shows the single-line diagram of Bay#1 and the fault scenarios at three points; node 1, node 2, and node 3, respectively. Fig. 5 illustrates the current waveforms of phase A of BB#1 for SLG in Bay#1. It is clear that the closer the fault point to BB#1 the higher the peak fault current. The figure shows that the first peak of the monitoring current at node 1 is -4492 A, at node 2 is -4669 A, and at node 3 is -6416 A.

Fig. 6 illustrates the current waveforms of phase A of BB#1 for SLG in Bay#7. It is clear that the closer the fault point to BB#1 the higher the peak fault current. The figure shows that the first peak of the monitoring current at node 1 is 12648 A, at node 2 is 13049 A, and at node 3 is 15767 A.

Fig. 7 illustrates the current waveforms of phase A of BB#1 for HIF in Bay#1. It is clear that the closer the fault point to BB#1 the higher the monitoring peak current. The figure shows that the first peak of the monitoring current at node 1 is 8 A and at node 2 is 17 A.

Fig. 8 illustrates the current waveforms of phase A of BB#1 for HIF in Bay#7. It is clear that the closer the fault point to BB#1 the higher the monitoring peak current. The figure shows that the first peak of the monitoring current at node 1 is 29 A and at node 2 is 35 A.

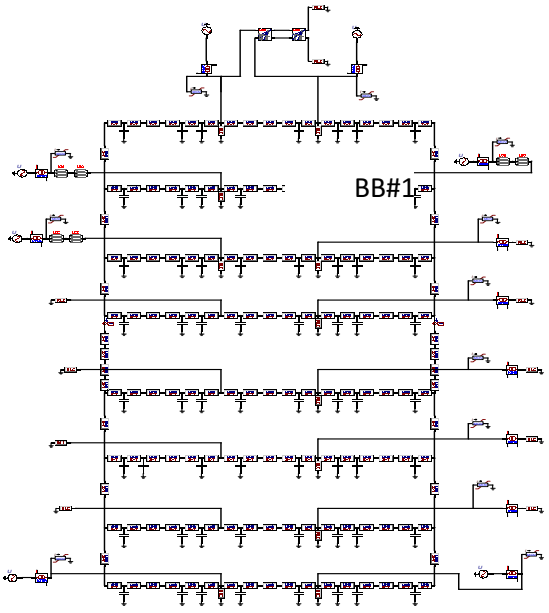

Fig. 2. ATP/EMTP model of Talkha 220 kV GIS

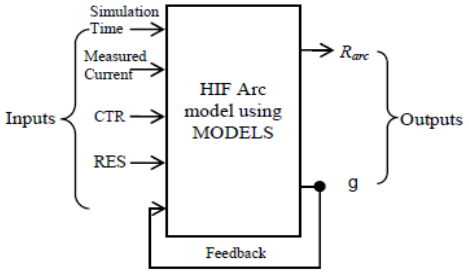

Fig. 3. The ATP/EMTP HIF Arc Model

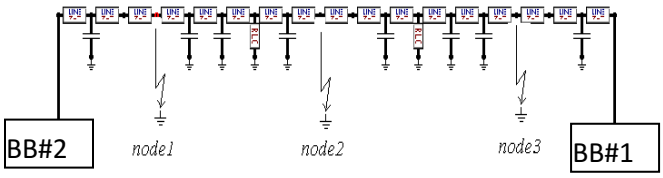

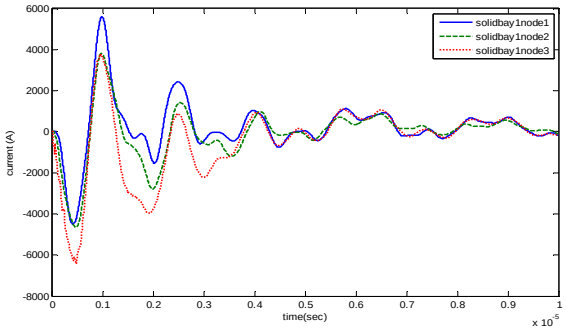

Fig. 5. Current waveforms of phase A of BB#1 at SLG fault on Bay#7

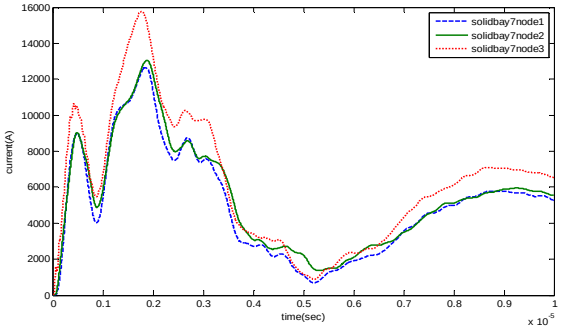

Fig. 6. Current waveforms of phase A of BB#1 at SLG fault on Bay#7

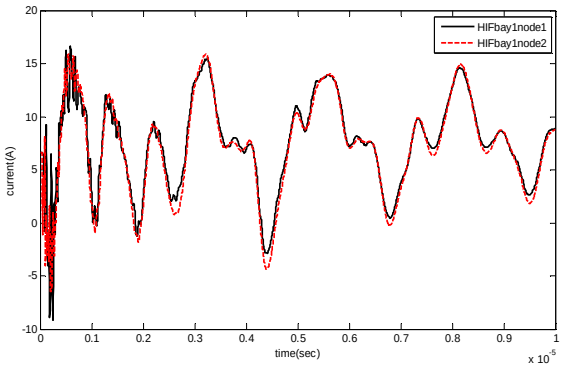

Fig. 7. Current waveforms of phase A of BB#1 at HIF on Bay#1

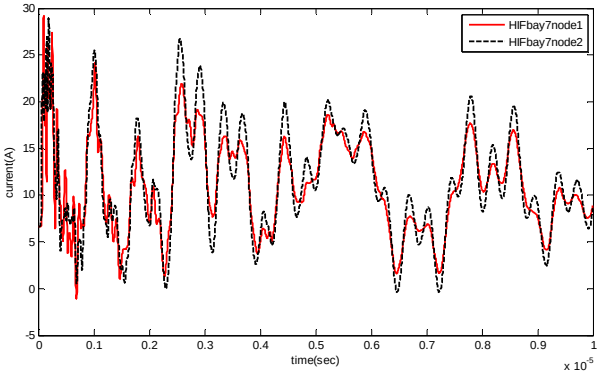

Fig. 8. Current waveforms of phase A of BB#1 at HIF on Bay#7

The current is measured in the middle of BB#1 near the bus tie. The most of generation units are located in the upper part of GIS; as shown in Fig. 2. It is noted that for the fault on Bay#7, all the generation units fed this fault, so the monitoring fault current at measuring point at the middle of BB#1 for both HIF and SLG is greater than that measured for Bay#1**.**

The Proposed ANN-Based Classifier

ANN have demonstrated the special capability of mapping the very complicated relationships between the inputs and the outputs and of revealing subtle differences in features between ill-defined patterns, particularly of the aforementioned types associated with wideband fault generated noise.

A large number of simulations are performed to generate a good representative data set for training and testing ANN. Once sets of training/testing patterns have been generated, the appropriate ANN architecture and associated parameters are chosen. The task of ANN is to learn to capture the fault type and location.

Multilayer feed forward network is the most widely used [13-14]. The back propagation algorithm is the most commonly used procedure yielding usually good generalization capabilities. Multilayer Feed forward networks consist of a series of layers. The first layer has a connection from the network input. Each subsequent layer has a connection from the previous layer. The final layer produces the network's output. Feed forward networks can be used for any kind of input to output. A feed forward network with hidden layer can fit any finite input-output mapping problem.

Various combinations of number of hidden layers and numbers of units are tested. The chosen ANN consists of one input layer with 144 neurons, a single hidden layer with 72 neurons, and only one output layer with one neuron; 1 for solidly to ground fault and 2 for high impedance to ground arc fault, as shown in Fig. 9.

The second step is to identify the fault location. A two parallel extended ANNs are designed to do the second function; one for the HIF and the other for the solidly fault to ground. Each of the two extended ANNs consists of one input layer with 72 neurons, a single hidden layer with 47 neurons, and only one output layer with one neuron (1 ~ 8 : code of faulted bay), as shown in Fig. 9. The proposed ANN is trained using part of the simulation results (270 inputs). The performance of the training is shown in Fig. 10. It is shown that the maximum proposed error is 0.001

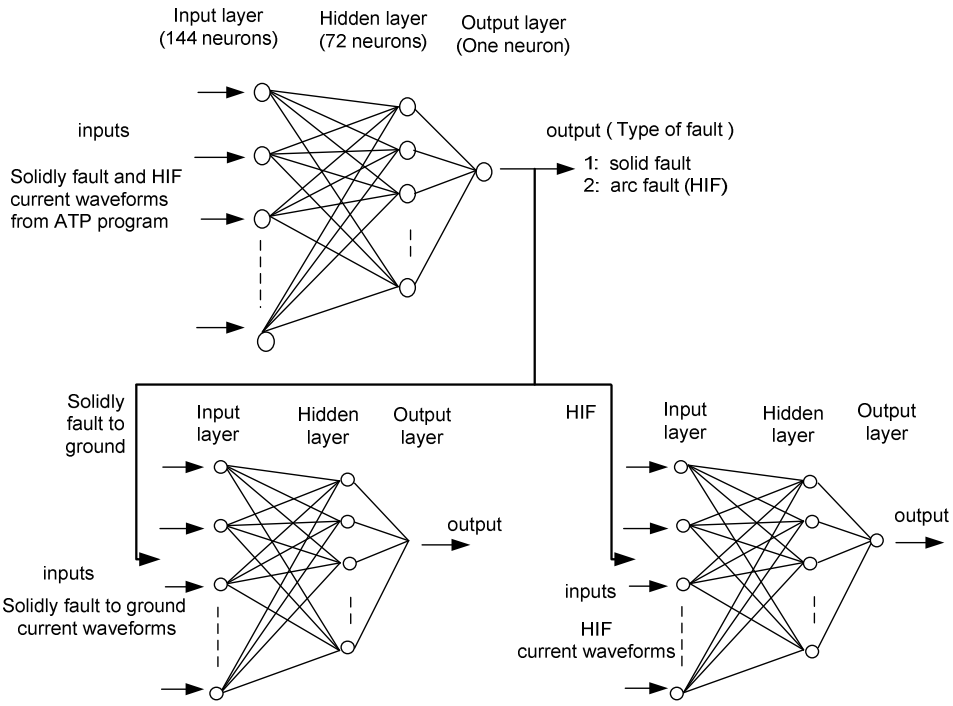

Fig. 9. Structure of the proposed multi-stage feed-forward ANN

6. Test Results

Following the training of ANN, a separate set of the simulation results (18 inputs) is supplied to the ANN in order to evaluate the validity of the proposed technique. Table 2 gives some examples of the results. The left column of the table is the fault type and the second column is the fault location. Then the last three columns are the desired outputs, the actual outputs, and the percentage error for fault type and fault location.

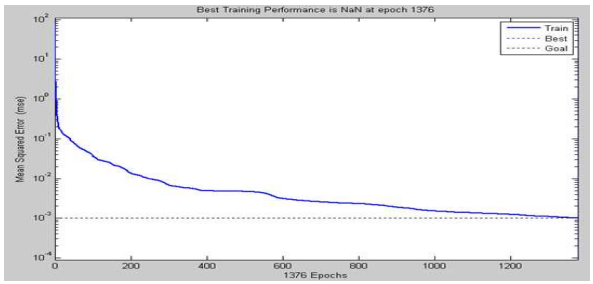

Fig. 10. Performance of the proposed ANN

It is evident from the results that, the proposed approach succeeds in detecting the fault in any bay of the GIS. The proposed approach depends on the measurement of only the current of one point in the GIS. The measurement point is selected in this study at the middle of BB#1; between Bay#4 and Bay#5. It is shown in Table 2 that the closer the fault point to the measuring point, the less the percentage error.

Table 2. The proposed ANN-Classifier Test Results

Fault		Desired Output		Actual Outputs		% Error	
Type	Location	Type	Location	Type	Location	Type	Location
SLG	Bay#1	1.0	1.0	1.0155	0.9494	1.55	5.06
	Bay#2	1.0	2.0	1.0041	1.9342	0.41	3.29
	Bay#3	1.0	3.0	1.0020	2.9898	0.20	0.3400
	Bay#4	1.0	4.0	1.0046	3.9768	0.46	0.3314
	Bay#5	1.0	5.0	1.0046	4.9894	0.46	0.212
	Bay#6	1.0	6.0	1.0005	5.9846	0.05	0.2566
	Bay#7	1.0	7.0	0.9989	6.9784	0.11	0.3085
	Bay#8	1.0	8.0	1.0033	7.9105	0.33	1.1187
HIF	Bay#1	2.0	1.0	1.9870	1.0248	0.65	2.4800
	Bay#2	2.0	2.0	2.0208	2.0380	1.04	1.900
	Bay#3	2.0	3.0	1.9758	2.9917	1.21	0.2767
	Bay#4	2.0	4.0	2.0253	3.9998	1.265	0.0005
	Bay#5	2.0	5.0	1.9931	5.0076	0.345	0.152
	Bay#6	2.0	6.0	2.0205	6.0099	1.025	0.165
	Bay#7	2.0	7.0	1.9267	6.9884	3.665	0.166
	Bay#8	2.0	8.0	2.0236	7.9703	1.18	0.371

Conclusions

In this paper, an ANN-based approach is proposed and designed to detect and classify faults in Talkha 220 kV GIS. The presented approach has the ability to detect the fault, classify the fault type, and identify the fault point. The layout of the Talkha GIS is modeled using ATP/EMTP. A multi-stages ANN of multilayer feed-forward network is designed, trained, and tested. The proposed approach accurately discriminates between the bolt ground faults and the high impedance faults, and identifies the faulted Bay. The proposed approach has distinct advantages; first of all, the high speed detection of the fault, also, the accurate identification of the fault point. The high speed of this approach is important in GIS which is considered critical in the electric power network and the accurate fault type classification leads to take the right protective actions

References

[1] P. Alves da silva, A. H. F.Insfran, P. M. da silverira, and G. Lambert-Torres, ‘’Neural Networks for Fault location in Substations’’, IEEE Transactions on Power Delivery, Vol. 11, No. 1, January 1996, pp. 234-241.

[2] J. A. Martinez, P. Chowdhuri, R. Iravani, A. Keri, D. Povh, “Modeling Guidelines for Very Fast Transients in Gas Insulated Substations”, IEEE Working Group on Modeling and Analysis of System Transients, IEEE Transactions on Power Delivery, Vol. 11, No. 4, October 1996, pp. .

[3] Mariusz Stosur, Marcin Szewczyk, Wojciech Piasecki, Marek Florkowski, Marek Fulczyk, “GIS Disconnector Switching Operation – VFTO Study”, Modern Electric Power Systems 2010, Wroclaw, Poland.

[4] K. Warwick, A. Ekwue, and R. Aggarwal, "Artificial Intelligence Techniques in Power Systems", IET, 1997, p. 302.

[5] ANN Toolbox for MATLAB, Math Works 2007.

[6] R. Aggarwal and Y. Song, “Artificial Neural Networks In Power Systems: I. General Introduction to Neural Computing,” Power Engineering Journal, Vol. 11, No. 3, pp. 129-134, 1997.

[7] R. Aggarwal and Y. Song, “Artificial Neural Networks in Power Systems: III. Examples of Applications in Power Systems,” Power Engineering Journal, Vol. 12, No. 6, 1998, pp. 279-287.

[8] M. Kondalu, Gillella Sreekanth Reddy, P. S. Subramanyam, “Estimation of Transient Over Voltages in Gas Insulated Bus Duct From 220 kV Gas Insulated Substation”, International Journal of Computer Applications, Volume 20, No. 8, April 2011, pp. 0975 – 8887.

[9] D. T. A. Kho, K. S. Smith, “Analysis of Very Fast Transient Overvoltages in a Proposed 275 kV Gas Insulated Substation”, International Conference on Power Systems Transients (IPST2011), Delft, Netherlands, June 14-17, 2011.
[10] J. V. G. Rama Rao, J. Amarnath, and S. Kamakshaiah. “Simulation and Measurement of Very Fast Transient Over Voltages in A 245 kV GIS and Research on Suppressing Method Using Ferrite Rings”, ARPN Journal of Engineering and Applied Sciences, Vol. 5, No. 5, May 2010, pp. .
[11] Kamal M. Shebl, Ebrahim A. Badran, and Elsaeed Abdalla “A Combined MODELS-TACS ATPdraw General Model of the High Impedance Faults in Distribution Networks”, The 14th International Middle East Power Systems Conference (MEPCON’10), Cairo University, Egypt, December 19-21, 2010, Paper ID 220.
[12] Stanislav Misak, “Mathematical Model of Electric Arc Respecting Mayr Theory in EMTP-ATP”, Acta Electrotechnica et Informatica, Vol. 8, No. 3, 2008, pp. 66–69.
[13] R. Aggarwal and Y. Song, “Artificial Neural Networks in Power Systems, II- Types of Artificial Neural Networks”, Power Engineering Journal, Vol. 12, No. 1, pp. 41-47, 1998.
[14] A. Ukil, “Intelligent Systems and Signal Processing in Power Engineering”, Springer, 2007.